Journal of Power Sources 224 (2013) 168–173

Contents lists available at SciVerse ScienceDirect

Journal of Power Sources

journal homepage: www.elsevier.com/locate/jpowsour

Improved performance of dye-sensitized solar cells by trace amount Cr-doped TiO_2 photoelectrodes

Yanan Xie [a], Niu Huang [a], Sujian You [a], Yumin Liu [a], Bobby Sebo [a], Liangliang Liang [a], Xiaoli Fang [a], Wei Liu [a,b], Shishang Guo [a,b,*], Xing-Zhong Zhao [a,b]

[a] School of Physical Science and Technology, Wuhan University, Hubei 430072, People's Republic of China
[b] Key Laboratory of Artificial Micro- and Nano-structures of Ministry of Education, School of Physics and Technology, Wuhan University, Wuhan 430072, People's Republic of China

HIGHLIGHTS

► The trace amounts of Cr-doped TiO_2 have been used for the dye-sensitized solar cells (DSSCs).
► The short-circuit photocurrent density and electron lifetime have increase–decrease trace.
► The overall energy conversion efficiency has increased to 6.35% with 50 ppm Cr-doped TiO_2.
► The electron transport property has enhanced significantly with Cr-doped TiO_2.

ARTICLE INFO

Article history:
Received 14 July 2012
Received in revised form
17 September 2012
Accepted 19 September 2012
Available online 9 October 2012

Keywords:
Dye-sensitized solar cells
Trace amount
Chromium-doped titanium dioxide
Hydrothermal method
Electron transport

ABSTRACT

Trace amount chromium-doped (Cr-doped) TiO_2 is prepared by hydrothermal method for dye-sensitized solar cells (DSSCs). The effect on photovoltaic performance of the cells is investigated via control of the concentrations of Cr doped in TiO_2. Rutile phase increases when Cr is incorporated into TiO_2 while the property of electron transport in photoelectrodes is improved by doping Cr which results in a reduced resistance (R_{ct}) of the electron transport within mesoporous layer and an improved electron lifetime. The regularity of R_{ct} and electron lifetime is reversed when the level of doped Cr exceeds 50 ppm. On the other hand, owing to the doping effect of Cr, the short-circuit photocurrent density (J_{sc}) of DSSCs is remarkably enhanced and reaches maximum. Consequently, the overall energy conversion efficiency enhances to 6.35% with Cr-doped TiO_2 of 50 ppm, which is 14.62% higher than that with undoped TiO_2. In general, compared with undoped TiO_2, Cr-doped TiO_2 is a better photoanode material and a more promising alternative for high efficient DSSCs.

1. Introduction

Dye-sensitized solar cell (DSSC) research is among the hot areas of current research in the field of materials for photoelectric energy conversion and nano technology [1–3]. Attributed to the advantages of low cost compared to commercial solar cells, simple production process and stable performance, DSSCs provide more effective method for human to use the solar energy cheaply and conveniently [4–6]. However, further improvement of the stability and photoelectric conversion efficiency of DSSC for industrialization is still a major issue for its application prospects. In the process of the photocurrent production in DSSCs, excited states dye molecules inject electrons into the conduction band (CB) of TiO_2, from which the electrons are transported into the back contact and then flow in the external circuit. At the same time, there are some recombination and traps caused by some electrons with tri-iodide of the electrolyte or oxidized dye. The two opposing electron paths are in rivalry and have an important effect on electron transport process and collection efficiency in the nanostructure TiO_2 film [7]. The improvement of charge-transfer ability is helpful to the short-circuit current density (J_{sc}) increase that could offer a great chance to improve the photoelectric conversion efficiency of DSSCs. Recently, several methods have been utilized to modify the structure of the working electrode (TiO_2 electrode) to improve the performance of DSSCs such as the improvement of J_{sc} by metal doping [8–15]. Cr-doped TiO_2 films or powders have been used as photocatalysts [16,17]. However, few studies have been reported about Cr-doped TiO_2 applied as photoanode of DSSCs. In recent

* Corresponding author. School of Physics and Technology, Wuhan University, Wuhan 430072, People's Republic of China. Tel.: +86 27 87642784; fax: +86 27 68752569.
E-mail address: gssyhx@whu.edu.cn (S. Guo).

0378-7753/$ – see front matter © 2012 Elsevier B.V. All rights reserved.
http://dx.doi.org/10.1016/j.jpowsour.2012.09.078

work, modification of Cr-doped nanostructure TiO_2 photoanode to improve the photovoltaic efficiency of a DSSC has been investigated [18]. The results showed that the double layer of Cr-doped and pure TiO_2 electrode acted as a diode. Additionally, the energy barrier prevented electron loss by repressing the recombination rate in order to enhance the J_{sc}. However, doping Cr is not the direct factor for the improvement of the DSSCs performance, besides the doping concentration level of several tens of parts per million (ppm) is never investigated for DSSCs.

In this work, we synthesized undoped and Cr-doped TiO_2 photoanodes with different Cr doping by hydrothermal reaction. The concentration levels of Cr doping were in ppm. The characteristics of different photoanodes were measured by XRD, SEM and UV–visible absorption. The Cr-doped TiO_2 is successfully applied as photoanode material in DSSCs. Furthermore, we report the relationship between Cr content and photovoltaic characteristics. It is demonstrated that Cr doping is favorable to electron transfer and improvement of J_{sc} that contribute to the significant improvement of the conversion efficiency of DSSCs. The mechanism of the improvement caused by Cr doping is also discussed.

2. Experiment section

2.1. Materials

Titanium isopropoxide (TTIP, $Ti[OCH(CH_3)_2]_4$) and chromium nitrate ($Cr(NO_3)_3\cdot 9H_2O$) were used as Ti and Cr precursors. Triton X-100 was selected as emulsifier of TiO_2 slurry. Polyethylene glycol (PEG, molecular weight of 20,000) was obtained from Sinopharm Chemical Reagent Corporation, China. Fluorine-doped SnO_2 conductive glass (FTO, sheet resistance 10–15 Ω sq^{-1}) was purchased from Asahi lass, Japan. The dye (N719) was purchased from Solaronix, Switzerland. Iodine (I_2, 99.8%) was obtained from Beijing Yili chemicals, China. Lithium iodide (LiI, 99%), guanidine thiocyanate (GNCS) and 4-tert-butylpyridine (TBP) were obtained from Acros. Propylene carbonate (PC) was obtained from Sinopharm Chemical Reagent Corporation (China). All the reagents used were analytical grade.

2.2. Preparation of Cr–TiO_2 and undoped TiO_2 slurries

The undoped and Cr-doped TiO_2 pastes were prepared by hydrothermal synthesis method. Typically, 10 mL of TTIP mixed with 2.1 g acetic acid was added drop-wise to 50 mL of deionized water mixed with different amounts of $Cr(NO_3)_3\cdot 9H_2O$ (Cr/TiO_2 molar ratio: 10 ppm, 30 ppm, 50 ppm, 70 ppm) under vigorous stirring for 1 h. Then 0.68 mL of nitric acid was added to the previous mixture solution and stirred for 3 h at 80 °C in order to obtain transparent sol. The transparent sol was filtered to remove insoluble impurities. Then the sol was heated at 220 °C in autoclave for 12 h and cooled down at room temperature, followed by addition of nitric acid (0.4 mL) and dispersion by sonication. The solution was then concentrated by rotary evaporator. Finally, PEG and Triton X-100 were added to form the Cr-doped TiO_2 slurry (Cr–T-1: 10 ppm Cr-doped TiO_2, Cr–T-2: 30 ppm Cr-doped TiO_2, Cr–T-3: 50 ppm Cr-doped TiO_2, Cr–T-4: 70 ppm Cr-doped TiO_2). The method for undoped TiO_2 slurry was similar to the above.

2.3. Preparation of photoelectrodes and DSSCs

The undoped and Cr-doped TiO_2 slurries were coated onto FTO substrates by doctor blade method, respectively, followed by calcination at 500 °C for 30 min. The process was repeated and the resulting transparent mesoporous layer of photoelectrodes (thickness of 8 ± 0.5 μm) was obtained. The mesoporous photoelectrodes were preheated at 120 °C for 30 min, after cooling down, they were immersed in a 0.5 mM ethanolic N-719 solution for 24 h at room temperature. The dye adsorbed photoelectrodes were rinsed with absolute ethanol to remove the redundant dye molecules. After drying the sensitized photoelectrodes, the sandwich-type DSSCs were assembled with an electrolyte layer containing 0.05 mM LiI, 0.03 M I_2, 0.1 M PMII (1-methyl-3-propyl imidazolium iodide), 0.1 M GNCS and 0.5 M TBP in mixed solvent of acetonitrile and PC (v/v = 1:4) between the photoelectrodes and Pt electrode prepared by sputtering method [19].

3. Results and discussion

3.1. Material characterization

3.1.1. XRD and morphologies

The XRD patterns of the undoped and Cr-doped TiO_2 powders calcined are shown in Fig. 1. It shows well-resolved diffraction peaks corresponding to the reflections of anatase TiO_2 material (JCPDS file no. 21-1272). It can clearly be seen that the rutile phase in the Cr-doped TiO_2, marked by the extra reflection at $2\theta = 27°$, corresponds to the (110) plane. However there is only a minor presence in undoped TiO_2 powder. It is indicated that the anatase-to-rutile phase transformation occurs from Cr doping.

Fig. 2(a) and (b) shows the SEM images of the undoped and Cr-doped TiO_2 films (Cr–T-3) after calcination, respectively. All the films have good crystallinity with particle size of 20–30 nm with typical porosity and good uniformity for DSSC. But the surface topography of the films is almost unchanged before and after modification of Cr doping.

3.1.2. UV–visible absorption and powders color

The UV–visible absorption spectra of undoped and Cr-doped TiO_2 films (Cr–T-3) are shown in Fig. 3. It is exhibited that the visible light adsorption of the Cr-doped TiO_2 films is slightly enhanced compared to the undoped TiO_2 film. It might be that owing to a downward movement of the conduction band edge of Cr-doped TiO_2, the band gaps of Cr-doped TiO_2 become slightly smaller than of undoped TiO_2. According to the UV–visible absorption spectra of undoped and Cr-doped TiO_2 films, the spectral response from Cr-doped TiO_2 can clearly be seen even though the concentration level is several tens of parts per million, which was observed similarly from others' work [20,21].

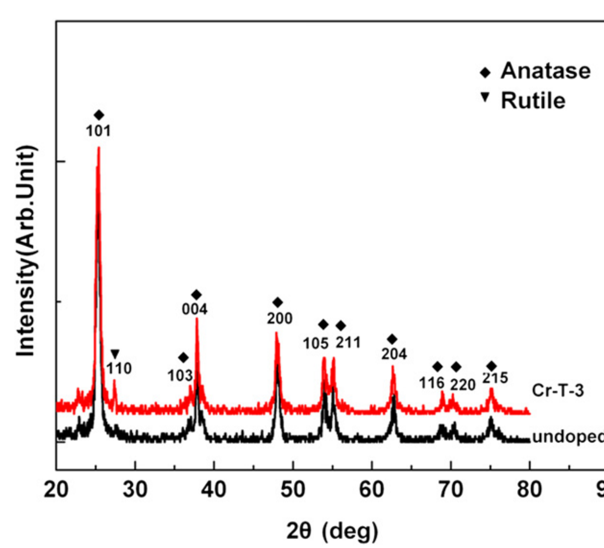

Fig. 1. XRD patterns of synthesized undoped and Cr–T-3 powders.

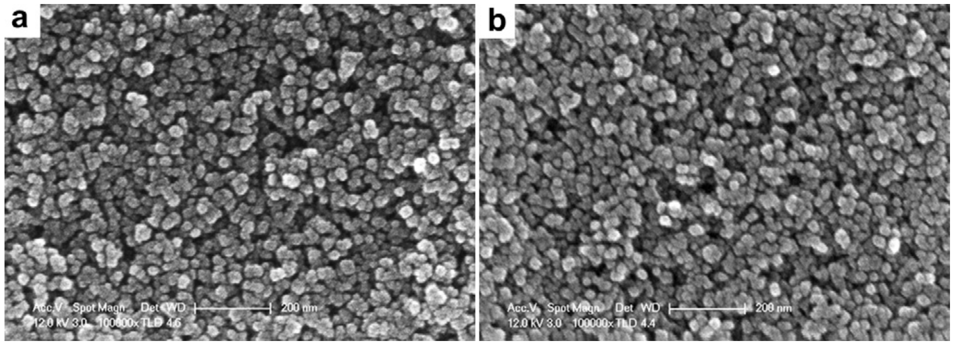

Fig. 2. SEM images (×100,000) of the surface morphology coated using undoped TiO_2 film (a) and Cr–T-3 film (b).

The powders based on undoped and Cr-doped TiO_2 are shown in Fig. 4 respectively. It can be seen clearly that the powder of undoped TiO_2 is white and the powder of Cr–T-3 is light yellow. We also synthesized some powders of Cr-doped TiO_2 (not shown here) which are orange, under the higher concentration level such as several parts per thousand by same method. It might be that Cr^{3+} is transformed to higher valence state of Cr^{6+} or Cr^{5+} under high temperature and pressure with heating at 220 °C in autoclave for 12 h, resulting in the transformation of color.

3.1.3. Dye desorption experiment

UV–vis spectra for dye solution desorbed from different photoelectrodes with same area (1 cm^2) and same thickness (8 ± 0.5 μm) are shown in Fig. 5(a). It can be indicated that absorption from undoped and Cr–TiO_2 photoelectrodes is similar from the characteristic absorption peak of N719 at about 500 nm. Absorption concentration is calculated and shown in Fig. 5(b). It is also found that the different photoelectrodes have similar dye loading as seen from the curve which may be due to similar morphology of different photoelectrodes shown by SEM images. Thus the amount of dye absorbed is unchanged by Cr doping.

3.2. J–V characteristics

Fig. 6 shows the J–V characteristics of the DSSCs and the photovoltaic performance parameters are summarized in Table 1 (0.87 sun) which shows the correlation between the photovoltaic performance parameters and the Cr content in the TiO_2. We can observe the fill factor (FF) nearly unchanged and some lightly extent the open-circuit voltage (V_{oc}) drop from different cells built using as different photoelectrodes. The V_{oc} decrease of Cr-doped TiO_2 compared to undoped TiO_2 is similar to the use of the same subgroup tungsten as a dopant in TiO_2 in dye-sensitized solar cells (DSSCs) [22], Additionally, it can be seen distinctly that increasing the concentration of Cr gives rise to the increase of the short-circuit photocurrent density (J_{sc}) from 10.02 mA cm^{-2} to a maximum of 11.34 mA cm^{-2} for 50 ppm doping level before a decline to 10.74 mA cm^{-2}. The energy conversion efficiency (η) increases gradually as the quantity of Cr and reaches an optimum value coinciding with Cr quantity of 50 ppm, after which the effect is reversed and η begins to fall. The energy conversion efficiency attains a maximum of 6.35% which is 14.62% higher than the undoped TiO_2. It can be seen from Table 1 that the variation in energy conversion efficiency and J_{sc}, respectively, follow the same trend. Although there is some rutile phase added as shown by XRD, which may lead to the low electron diffusion coefficient and the decreased performance of DSSCs [23,24], the increase of energy conversion efficiency further indicates the effect of doping Cr for J_{sc}.

The enhancement of the electron-transfer ability can be discussed on the basis of the theoretical model of the electrical conductivity, which is based on the equation [10]

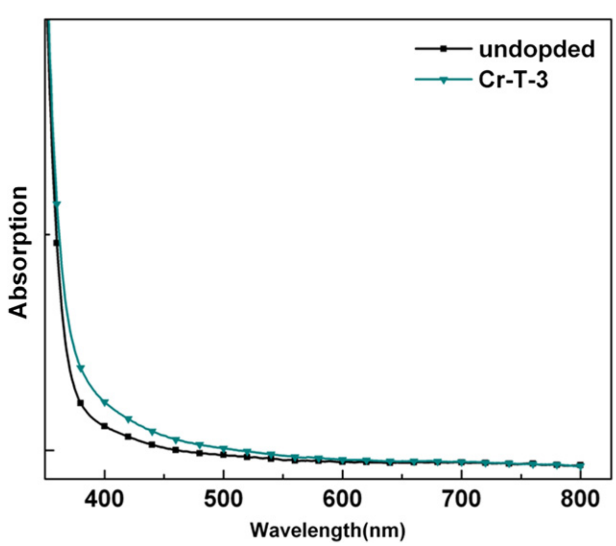

Fig. 3. UV–visible absorption spectra of undoped TiO_2 and Cr–T-3 films.

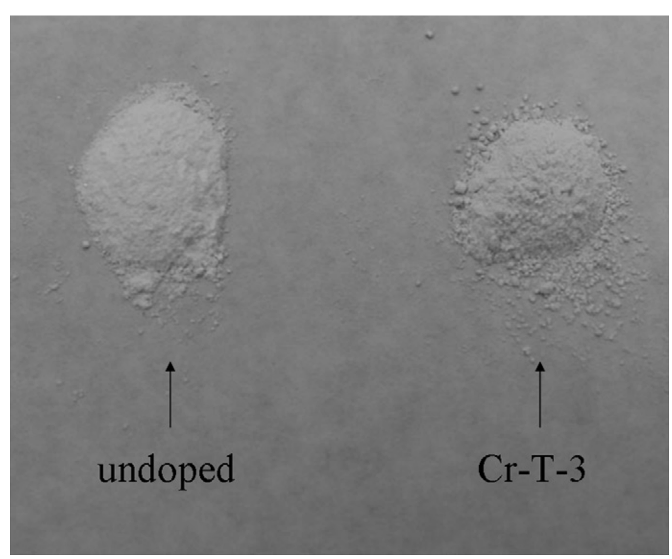

Fig. 4. The color change of powders after Cr doping.

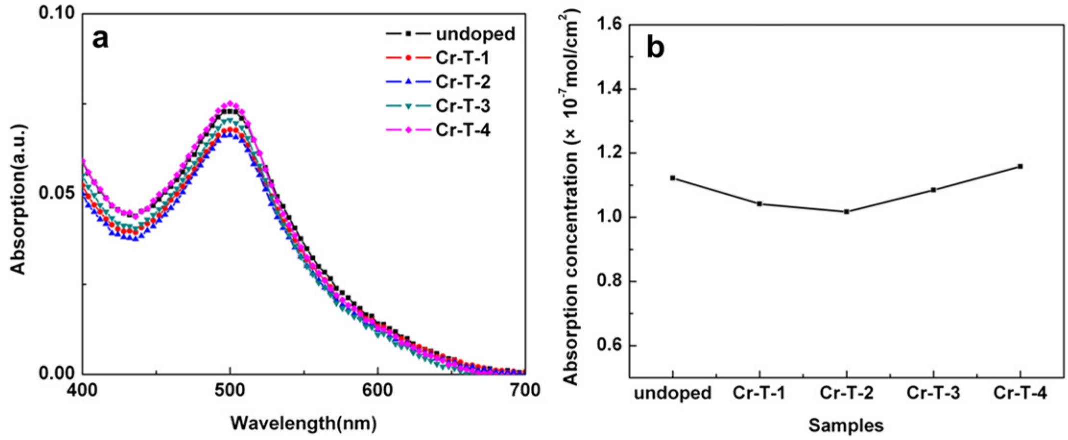

Fig. 5. (a) Dye absorbance from desorption experiment of undoped and Cr-doped TiO_2. (b) Dye absorption concentration of different samples.

$$\sigma = ne\mu \quad (1)$$

where e denotes the elementary charge, n is the electron concentration, and μ is the electron mobility, respectively. If n increases, the electron conductivity will be enhanced. However, the electron mobility will be decreased at high n due to the electron scattering defects [10]. Furthermore, a single electron injected in a 20-nm-sized particle produces an electron concentration of 2.4×10^{17} cm^{-3} [25]. There are $Ti^{4+}$of 9.95×10^{21} per 1 cm^3 TiO_2 according to the density of normal nano TiO_2 film ($\sim$1.2 g cm^{-3}) [26]. If an electron is injected in TiO_2 by Cr^{n+}, the electron concentration added by Cr doping of 50 ppm will be 4.98×10^{17} cm^{-3} in theory. So the level of electron concentration is the same as above (2.4×10^{17} cm^{-3}) which indicates the concentration levels of chromium doping are reasonable in our work. In addition, the increase of electron concentration enhances the electron-transfer ability and results in the improvement of the photocurrent density. However, severe defects increase charge recombination and the electron-transport efficiency decreased rapidly at high defect concentration, so J_{sc} decreases when the doping content is increased above 50 ppm. Consequently, Cr content of 50 ppm becomes dominant factor for J_{sc}.

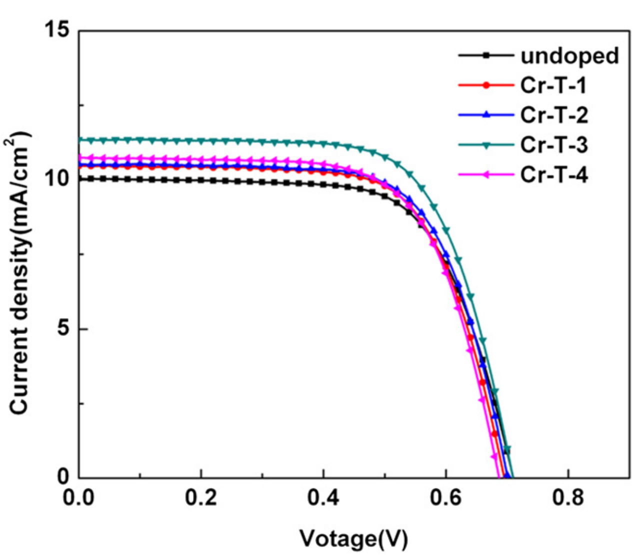

Fig. 6. J–V characteristics of DSSCs based on the undoped and Cr-doped TiO_2 photoanodes measured under simulated 0.87 sun.

3.3. EIS and OCVD analysis

The modeled internal resistances of the DSSCs based on five different photoelectrodes are illustrated via electrochemical impedance spectroscopy (EIS) shown in Fig. 7. The resistance (R_{ct}) of the electron transport within each mesoporous layer [23,27–29] indicated by the large semicircle in Fig. 7, is listed in Table 1. R_{ct} remarkably decreases with increasing Cr content and ultimately increases with further Cr doping. The smallest R_{ct} is achieved when Cr content is 50 ppm, which promotes more efficient charge transport in the mesoporous layer. Owing to the sites of recombination and severe defects introduced when there is too much Cr doping, the recombination speed within mesoporous layer dominates the charge transfer processes. Therefore, the value of R_{ct} should become large when 50 ppm of Cr doping exceeds. In other words, the charge transfer resistance in mesoporous layer by appropriate Cr doping is decreased, leading to a positive influence on the improvement of solar cell performance.

In order to further confirm the conclusion above, herein, we have investigated the influence of lifetime of electrons in the TiO_2 electrode as well as the performance of the DSSCs under varying the amounts of Cr content in the TiO_2 electrode by the open-circuit voltage decay (OCVD) measurement shown in Fig. 8. The OCVD reflects the electron lifetimes and recombination in DSSCs [25] which can be derived as a function of photovoltage by the photovoltage transient decay technique under open-circuit conditions. Fig. 8 shows the electron lifetime calculated from OCVD spectra of DSSCs based on the undoped and Cr-doped TiO_2 photoanodes. The electron lifetime is calculated by the formula [30]

$$\tau = \frac{k_B T}{e}\left(\frac{dV}{dt}\right)^{-1} \quad (2)$$

In the measurement of OCVD, during the decay of V_{oc}, electron concentration evolves from the initial steady state value to

Table 1
Performance of DSSCs based on undoped and Cr-doped TiO_2 photoanodes.

DSSCs	Doping (ppm)	V_{oc} (V)	J_{sc} (mA cm^2)	FF	η (%)	R_{ct} (Ω)
Undoped	0	0.706	10.02	0.68	5.54	17.40
Cr–T-1	10	0.696	10.50	0.68	5.71	17.36
Cr–T-2	30	0.701	10.57	0.68	5.81	17.02
Cr–T-3	50	0.705	11.34	0.69	6.35	14.8
Cr–T-4	70	0.688	10.74	0.67	5.71	18.3

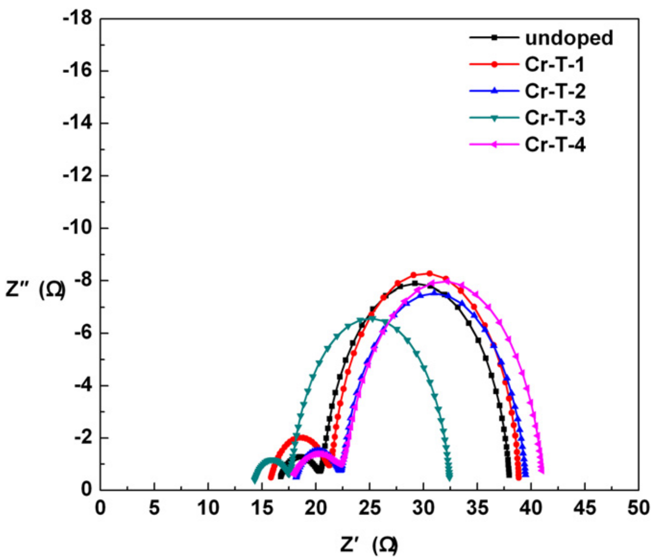

Fig. 7. EIS of DSSCs based on the undoped and Cr-doped TiO_2 photoanodes measured in the illumination at the applied bias of V_{oc}.

the dark equilibrium ($V_{oc} = 0$) with concentration n_0. We will generally neglect the final region of decay at $V_{oc} \approx 50$ mV or less, which is poorly resolved in the current setup, hence we can assume that $n \ll n_0$, V decreases by about 0.6 V, which is in agreement with previously reported values obtained by IMVS [31]. So we adapted to the curve of the electron lifetime for different photoanodes above 0.6 V, which was shown via inset figure in Fig. 8. It can be observed that the lifetime of electron increases with the doped Cr content and reaches the longest value for Cr–T-3. The trend of electron lifetime is consistent with EIS results. The presence of Cr-doped TiO_2 increases the electron lifetime and makes the electron transfer more easily. The lower the resistance for electron transport, the longer the lifetime as implied by OCVD, thus favoring the charge collection rate of photogenerated electrons [32], which led to the highest energy conversion efficiency of Cr–T-3.

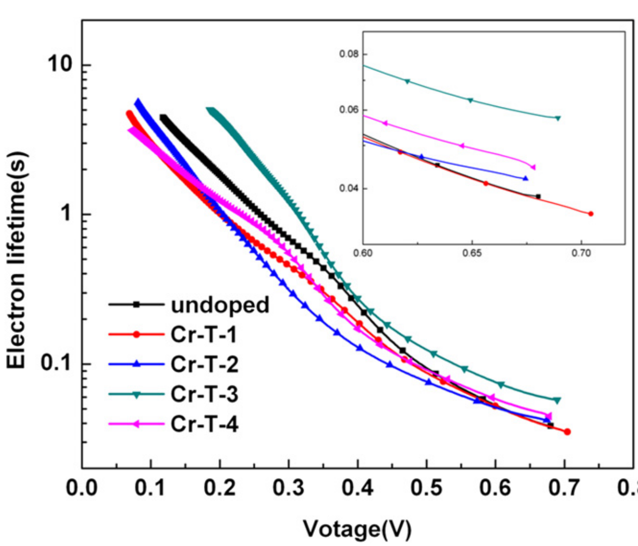

Fig. 8. The electron lifetime calculated from OCVD spectra of DSSCs based on the undoped and Cr-doped TiO_2 photoanodes.

4. Conclusion

In summary, we have developed a methodology of photoelectrode modification by Cr doping for DSSCs. Studies implied that the Cr additions offers more electron for TiO_2 and increases the property of electron transport for DSSCs. Although rutile phase is added in Cr-doped TiO_2 compared with undoped TiO_2. The J_{sc} and electron lifetime follow the same trend and increase with the increase of Cr addition and reaches the largest value when Cr-doped content is 50 ppm. Furthermore, the resistance (R_{ct}) of the electron transport within mesoporous layer decreases with increasing Cr addition and attains the smallest value of 14.8 Ω at 50 ppm of Cr doping. When the content of Cr is more than 50 ppm, the value of J_{sc}, electron lifetime and R_{ct} exhibit reverse trend owing to electron scattering by the defects at high defect concentration which is attributed to increased content of Cr doping. Our experimental results reveal that the optimal Cr content is around 50 ppm and the Cr–T-3 DSSC shows the best performance with the largest J_{sc} of 11.34 mA cm^{-2} and the largest photoelectric conversion efficiency of 6.35%, respectively. These results strongly indicate that 50 ppm Cr-doped TiO_2 based DSSC has a better conversion performance than undoped TiO_2 DSSC.

Acknowledgments

This work was supported by the National Natural Science Foundation of China (Grant Nos: 51132001, 51272184 and 10904117). The financial support of the National Basic Research Program of China (Grant No: 2011CB933300) was also acknowledged.

References

[1] A. Hagfeldt, G. Boschloo, L.L. Sun, L. Kloo, H. Pettersson, Chem. Rev. 110 (2010) 6595–6663.
[2] M. Grätzel, Acc. Chem. Res. 11 (42) (2009) 1788–1798.
[3] Q.D. Tai, X.Z. Zhao, F. Yan, J. Mater. Chem. 20 (2010) 7366–7371.
[4] B. O'Regan, M. Grätzel, Nature 353 (1991) 737–740.
[5] M.K. Nazeeruddin, A. Kay, I. Rodicio, R.H. Barer, E. Muller, P. Liska, N. Vlachopoulos, M. Grätzel, J. Am. Chem. Soc. 115 (1993) 6382–6390.
[6] M. Grätzel, Nature 414 (2001) 338–344.
[7] H.J. Snaith, R. Humphry-Baker, P. Chen, I. Cesar, M. Grätzel, Nanotechnology 19 (2008) 1–12.
[8] J. Navas, C. Fernandez-Lorenzo, T. Aguilar, R. Alcantara, J. Martın-Calleja, Phys. Status Solidi A 209 (2) (2012) 378–385.
[9] G.X. Xie, Y.L. Wei, L.Q. Fan, J.H. Wu, J. Phys. Conf. Ser. 339 (2012) 1–4.
[10] X.J. Lu, X.L. Mou, J.J. Wu, D.W. Zhang, L.L. Zhang, F.Q. Huang, F.F. Xu, S.M. Huang, Adv. Funct. Mater. 20 (2010) 509–515.
[11] A.K. Chandiran, F. Sauvage, M. Casas-Cabanas, P. Comte, S.M. Zakeeruddin, M. Graetzel, J. Phys. Chem. C 114 (2010) 15849–15856.
[12] Q.H. Yao, J.F. Liu, Q. Peng, X. Wang, Y.D. Li, Chem. Asian J. 1 (2006) 737–741.
[13] C.N. Zhang, S.H. Chen, L.E. Mo, Y. Huang, H.J. Tian, L.H. Hu, Z.P. Huo, S.Y. Dai, F.T. Kong, X. Pan, J. Phys. Chem. C 115 (2011) 16418–16424.
[14] P. Hasin, M.A. Alpuche-Aviles, Y.G. Li, Y.Y. Wu, J. Phys. Chem. C 113 (17) (2009) 7456–7460.
[15] Y. Zhang, L.L. Wang, B.K. Liu, J.L. Zhai, H.M. Fan, D.J. Wang, Y.H. Lin, T.F. Xie, Electrochim. Acta 56 (2011) 6517–6523.
[16] J.C. Yu, G.S. Li, X.C. Wang, X.L. Hu, C.W. Leung, Z.D. Zhang, Chem. Commun. 25 (2006) 2717–2719.
[17] H. Irie, T. Shibanuma, K. Kamiya, S. Miura, T. Yokoyama, K. Hashimoto, Appl. Catal., B: Environ. 96 (2010) 142–147.
[18] C. Kim, K.S. Kim, H.Y. Kim, Y.S. Han, J. Mater. Chem. 18 (2008) 5809–5814.
[19] C.H. Zhou, H. Hu, Y. Yang, B.L. Chen, J. Zhang, S.J. Wu, S. Xu, X.D. Xiong, H.W. Han, X.Z. Zhao, J. Appl. Phys. 104 (2008) 1–6.
[20] S.M. Karvinen, Ind. Eng. Chem. Res. 42 (2003) 1035–1043.
[21] E. Borgarello, J. Kiwi, M. Grätzel, E. Pelizzetti, M. Visca, J. Am. Chem. Soc. 104 (1982) 2996–3002.
[22] X. Zhang, S.T. Wang, Z.S. Wang, Appl. Phys. Lett. 99 (2011) 1–3.
[23] K.M. Lee, V. Suryanarayanan, K.C. Ho, Sol. Energy Mater. Sol. Cells 91 (2007) 1416–1420.
[24] N.G. Park, J. vande Lagemaat, A.J. Frank, J. Phys. Chem. B 104 (2000) 8989–8994.
[25] H.J. Agrell, G. Boschloo, A. Hagfeldt, J. Phys. Chem. B 108 (2004) 12388–12396.
[26] P.M. Sommeling, B.C. O'Regan, R.R. Haswell, H.J.P. Smit, N.J. Bakker, J.J.T. Smits, J.M. Kroon, J.A.M. van Roosmalen, J. Phys. Chem. B 110 (2006) 19191–19197.

[27] Q. Wang, J.E. Moser, M. Grätzel, J. Phys. Chem. B 109 (31) (2005) 14945–14953.
[28] N. Huang, Y.M. Liu, T. Peng, X.H. Sun, B. Sebo, Q.D. Tai, H. Hu, B.L. Chen, S.S. Guo, X.Z. Zhao, J. Power Sources 204 (2012) 257–264.
[29] Y.H. Jang, X.K. Xin, M. Byun, Y.J. Jang, Z.Q. Lin, D.H. Kim, Nano Lett. 12 (2012) 479–485.
[30] J. Bisquert, A. Zaban, M. Greenshtein, I. Mora-Sero, J. Am. Chem. Soc. 126 (41) (2004) 13550–13559.
[31] A. Zaban, M. Greenshtein, J. Bisquert, Chem. Phys. Chem. 4 (2003) 859–864.
[32] Y.Z. Zheng, X. Tao, L.X. Wang, H. Xu, Q. Hou, W.L. Zhou, J.F. Chen, Chem. Mater. 22 (2010) 928–934.